Kinetic Growth Instabilities on Vicinal Si(001) Surfaces

C. Schelling, G. Springholz, and F. Schäffler
Universität Linz, Institut für Halbleiterphysik, A-4040 Linz, Austria
(Received 16 February 1999)

We report new types of kinetic growth instabilities during silicon homoepitaxy on vicinal Si(001) surfaces with miscut angles $\leq 2°$. They occur under frequently employed growth conditions in an extensively studied material system. The characteristic features are (i) kinetic step bunching at low growth temperatures, (ii) a macroscopic zigzag morphology of $\langle 110 \rangle$ segments at intermediate temperatures, and (iii) a smooth, noncorrelated morphology at high growth temperatures and after annealing. A qualitative model is discussed that relates the morphological features with the kinetics of step incorporation and diffusion in connection with a symmetry-breaking miscut.

PACS numbers: 68.35.Bs, 61.16.Ch, 81.15.Hi

The technical relevance of Si(001) surfaces and interfaces for the performance of semiconductor devices, and the scientific interest in their intriguing surface properties have led to many static [1–3] and dynamic [4,5] surface studies. The latter became possible through epitaxial growth techniques with atomic layer precision, which were also a prerequisite for the commercial introduction of SiGe heterodevices [6]. New developments aim toward an exploitation of self-organized growth phenomena for the fabrication of low-dimensional quantum devices [7].

The spontaneous formation of surface corrugations during heteroepitaxial growth is commonly associated with mechanical stress induced by a lattice mismatch [8,9]. In contrast, here we report highly periodic surface morphologies of homoepitaxial films on vicinal Si(001) surfaces which result from purely kinetic mechanisms. They disappear upon annealing, whereas stress-driven phenomena [8] are equilibrium effects [9]. With lateral periods of 0.1–0.5 μm, and amplitudes of up to 20 Å, the surface corrugations should strongly affect the transport of carriers confined to such a surface or interface [10]. The observed pattern formation has as yet escaped detection, mainly because it occurs at epilayer thicknesses of several hundred atomic layers, which have rarely been investigated by scanning probe techniques in this material system [11,12].

The samples were grown by molecular beam epitaxy (MBE) in a two-chamber Riber SIVA 45 machine [13] at a residual gas pressure in the 10^{-10} Torr range. Substrates were 15–25 Ω cm p-type Si(001) with an epigrade surface finish and defined miscuts of 1.16° and 1.95° in a [100] direction, and of 1.58° in an approximate [110] direction. Miscut angles were determined to an accuracy of $\leq 0.05°$ by diffraction and specular surface reflection of the x-ray beam in a triple axis diffractometer. To ensure identical miscuts, the wafers were diced into 18×18 mm^2 samples, and only samples from the same wafer were employed for each experimental series. The samples were precleaned in an HF-free RCA process to avoid artifacts due to HF-induced hydrocarbon contaminations. The samples were mounted in all-Si adapters and radiatively heated. Temperature reading and control had been calibrated [13] to ± 15 °C. Prior to growth, the oxide was desorbed *in situ* at 1000 °C for 6 min. Initially, a Si buffer layer was deposited at 750 °C, but was later omitted, because it had no effect on the low-temperature morphology. The epilayers were deposited under typical Si MBE conditions at substrate temperatures between 350 and 750 °C, and growth rates between 0.2 and 0.8 Å/s.

The surfaces were characterized immediately after growth in air with a Park Scientific atomic force microscope (AFM) in contact mode, employing sharpened Si_3N_4 or Si cantilevers. Control experiments were conducted to rule out any artifacts due to factory wafer finish, chemical pretreatment, or thermal oxide desorption: After each of these steps the surfaces were found featureless with root-mean square (rms) roughnesses of a few monoatomic layers (1 ML = 1.35 Å). The surfaces are stable in air for several hours before signs of local oxidation become noticeable by AFM. The AFM data were statistically evaluated via line scans, two-dimensional fast Fourier transforms (FFT), and autocorrelation analyses.

Figure 1 shows a series of 5×5 μm^2 AFM micrographs from 2000 Å thick Si epilayers grown at 450, 490, and 550 °C at 0.8 Å/s on substrates with 1.16° miscut in a [100] direction. In this narrow temperature range the morphology undergoes a dramatic metamorphosis: At 450 °C the surface shows a regular terrace structure perpendicular to the miscut direction with an average spacing of 0.15 μm and a height of a few ML. The period is about a factor of 20 larger than the terrace width of evenly distributed ML steps at this miscut angle. The slightly undulating pattern is characteristic of the low-temperature growth regime and was followed down to 350 °C. The FFT (inset) and autocorrelation analyses confirm the high degree of order and the miscut-induced twofold symmetry. At 490 °C the terrace structure is still present, but it is now decorated with triangular features. These line up with a high degree of perfection along the miscut direction, forming periodic ridges perpendicular to the terraces. The periods in and perpendicular to the miscut direction

 © 1999 The American Physical Society

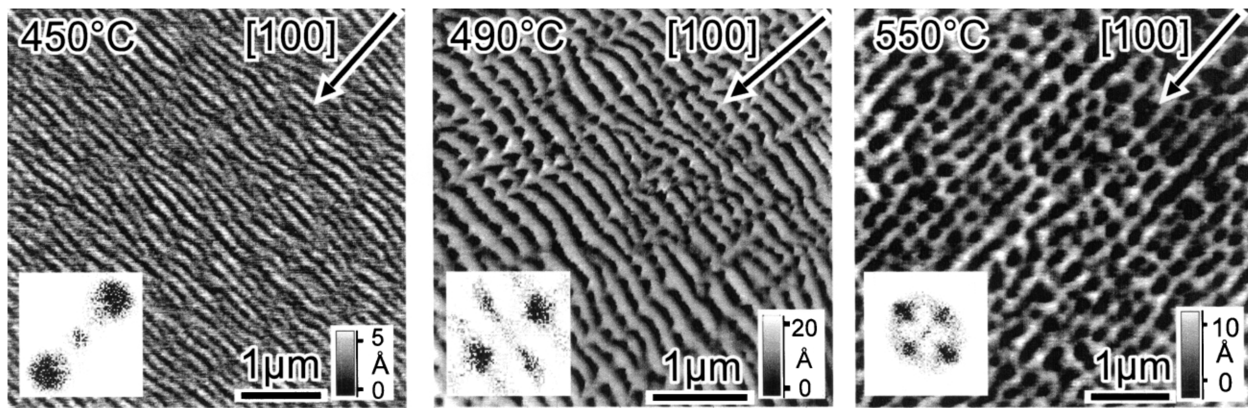

FIG. 1. $5 \times 5\ \mu m^2$ AFM images of 2000 Å thick homoepitaxial layers deposited on Si(001) surfaces with a miscut of 1.16° in [100] direction (arrows). Films were deposited at 0.8 Å/s and substrate temperatures of 450, 490, and 550 °C. Insets depict the two-dimensional Fourier transforms.

are comparable, leading to the distorted fourfold symmetry in the FFT (inset). The fainter features arise from the sides of the triangles. At 550 °C the FFT still reveals a high degree of order both in and perpendicular to the miscut direction, but the triangles have merged into extended ridges.

To study the influence of the miscut azimuth we performed experiments on substrates with a 1.58° miscut along an in-plane axis 10° off [110]. An example is shown in Fig. 2(b) in comparison with a [100] miscut sample. Both layers were deposited at 490 °C and 0.2 Å/s to a thickness of 1000 Å. In either case the terraces run perpendicular to the respective miscut direction, but the ledges disintegrate into zigzag arrangements of ⟨110⟩ segments. For the exact [100] miscut [Fig. 2(a)], symmetric right triangles form, which become acute upon rotation of the miscut direction; the acute angle is that between the miscut azimuth and the nearest ⟨110⟩ direction.

Initially, the height of the morphological features in Figs. 1 and 2 increases with film thickness. It takes 350 Å to clearly observe them by AFM, but no simple scaling behavior applies, as the amplitude saturates at a film thickness of about 1000 Å. Figure 3 shows the saturated peak-to-valley height and the average period width in miscut direction vs growth temperature for growth rates of 0.2 and 0.8 Å/s. The most prominent feature is the abrupt increase of the amplitude by more than a factor of 3, which occurs as the triangles appear on the terraces. For the [100] miscut the period width in the miscut direction gradually increases with growth temperature, but remains essentially constant at about 0.12 μm for the [110] miscut samples [compare Figs. 2(a) and 2(b)]. Beyond 550 °C the feature height decreases rapidly, and a lateral periodicity can no longer be extracted. Layers grown above 650 °C show a featureless rms roughness of 2 to 4 Å.

The maximum period lengths and rms feature heights depend surprisingly little on the growth rate in the range studied here. However, as expected of a kinetic phenomenon, the temperature range in which the triangle morphology occurs shifts to lower temperatures as the growth rate is reduced (Fig. 3). Also, at 0.2 Å/s the triangles become exceptionally regular [Fig. 2(a)].

There is a distinct dependence of the morphology on the miscut angle: Control experiments on almost

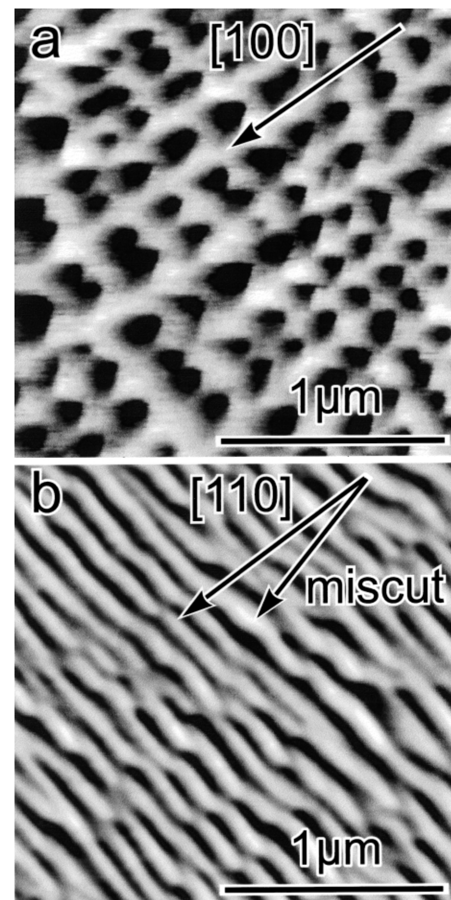

FIG. 2. $2 \times 2\ \mu m^2$ AFM images of 1000 Å thick Si epilayers deposited at 490 °C and 0.2 Å/s. (a) 1.16° miscut in [100]; (b) 1.58° miscut in a direction 10° off [110]. Gray scale is from 0 to 20 Å.

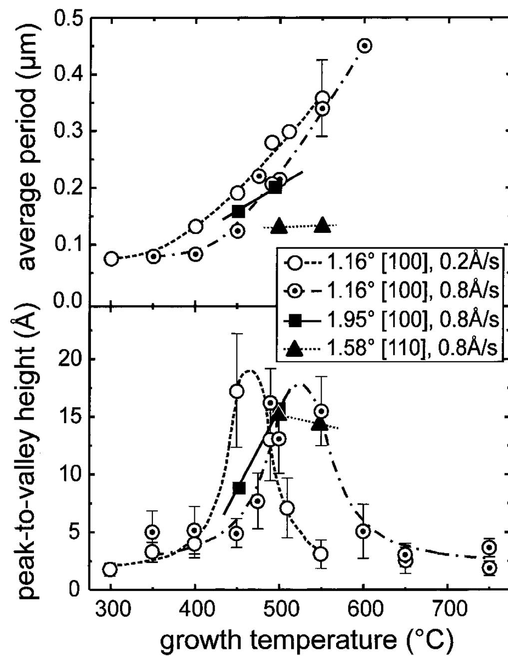

FIG. 3. Average period length in miscut direction and average peak-to-valley height of the morphological features versus growth temperature. Samples with 1.16° and 1.95° miscut in [100] and of 1.58° in the [110] direction are shown for growth rates of 0.2 or 0.8 Å/s. Curves are guides only.

singular (001) substrates (miscut $<0.12°$) showed smooth surfaces in the temperature range at about 500 °C, where the maximum amplitude occurs on miscut substrates. The experiments on 1.95° miscut samples (Fig. 3) fit the general behavior of the 1.16° miscut samples.

To assess thermal stability, a sample was grown at 490 °C and annealed *in situ* at 750 °C for 17 h, and another at 400 °C, with a 68 h anneal at 550 °C. In both cases a featureless surface resulted, with an rms roughness of about 2 Å. Obviously, both the low-temperature step-bunching regime and the ⟨110⟩ segmentation at about 500 °C are of pure kinetic origin. In addition, RHEED (reflection high energy electron diffraction) experiments showed that all layers were deposited under step-flow growth conditions.

While strain-induced step bunching in the Si/SiGe system is reasonably well understood [9,14], theoretical treatments of kinetic growth instabilities are as yet restricted to simple model surfaces with isotropic diffusion and ML steps. These act as perfect sinks for adatoms, but an Ehrlich-Schwoebel energy barrier (ESB) [15] makes the crossing of adatoms from the upper to the lower terrace a thermally activated process. A small ESB allows step-flow feeding from the upper terrace, which causes kinetic step bunching along the miscut direction [15]. Stable step flow always requires a finite ESB, which, in turn, is associated with the lateral Bales-Zangwill growth instability that leads to ridge formation perpendicular to the ledges [16].

The symmetry-breaking (2×1) dimer reconstruction [2] of Si(001) complicates the growth kinetics. It causes two types of monoatomic steps, namely, S_A steps parallel and S_B steps perpendicular to the ⟨110⟩ oriented dimer rows of the respective upper terrace [2]. The ESBs are believed to be small for both steps, but at low temperatures only S_B steps resemble perfect sinks for adatoms [17]. Also, the activation energy for diffusion along the dimer rows is lower than that for perpendicular motion [18]. For miscuts in a ⟨110⟩ direction these asymmetries cause the formation of D_B double steps under low-temperature growth conditions [19], as the faster S_B steps catch up with their down-step S_A neighbors. In thermal equilibrium, and for miscuts $<2.5°$, the single height steps prevail due to the stress fields associated with the reconstruction [3]. For a [100] miscut both dimer directions are under 45° to the miscut, which causes mixed-type ML steps with equally long S_A and S_B segments [20].

The temperature dependence of the surface morphology during growth reflects the interplay between diffusion, step incorporation, and the respective ESBs, which are all thermally activated processes. Unfortunately, the respective activation energies and sticking coefficients are not well known, and also the film thicknesses and the unusually large period widths are presently beyond the capabilities of Monte Carlo simulations. Nonetheless, our experimental results allow a qualitative assignment of the dominating mechanisms in the respective temperature ranges.

(i) Under low-temperature step-flow conditions the small ESBs of S_A and S_B steps cause kinetic step bunching [21] independently of the relative orientation between the miscut azimuth and the dimer row orientation. This mechanism is rather ineffective, since the observed period lengths involve typically 20 equilibrium terraces, whereas the modulation heights are just 4–5 ML. This indicates the formation of D_B steps under the prevailing nonequilibrium growth conditions [3,19], which have been associated with a stabilizing ESB [22].

(ii) In an intermediate temperature regime the probability of adatom incorporation into S_A and S_B steps has to become comparable. Since adatoms bond preferentially to kink sites, step incorporation is strongly correlated with the respective activation energies for kink formation [18]. As these differ by about 100 meV [17], the average kink separation on an S_A step is an order of magnitude larger at 300 °C, but approaches that of an S_B step to within a factor of 2–3 at 600 °C. A similar trend has been estimated for the anisotropy of the diffusion constant parallel and perpendicular to the dimer rows [17,23]. Consequently, a temperature range should exist [24], where S_A and S_B steps coexist with the stabilizing D_B steps. This would allow the observed formation of macroscopic features with the microscopic symmetry of the (2×1) reconstructed Si(001) surface, as is sketched in Fig. 4 for a miscut in [100] direction. Here an attempt is made to maximize the length of the D_B steps that define and stabilize the shorter sides of the macroscopic

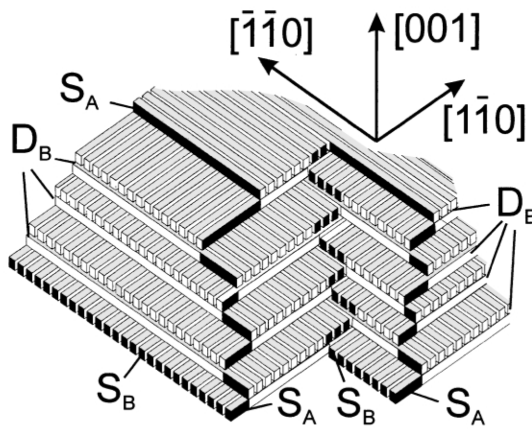

FIG. 4. Proposed microscopic structure of the triangle morphology maximizing the length of D_B steps. Cuboids represent the dimer rows. Note the zigzag arrangements of S_A (solid) and S_B (dotted) steps along the tips and at the intersection of the triangular prisms, which are topologically required.

triangles. While a vicinal surface with [110] miscut can be constructed entirely from D_B steps, the symmetry of the diamond lattice demands in the case of a [100] miscut additional S_A and S_B segments along the tips and the concave intersections of the triangles. Such a configuration can only be stable in a step-coexistence regime: At lower temperatures, when the S_B steps move much faster, the train of S_B segments in the concave portions prevents the development of macroscopic triangles.

(iii) At high temperatures the D_B steps become unstable [3], and the macrosteps disintegrate into the short zigzag chains of mixed S_A/S_B character observed in previous experiments [20]. This equilibrium state is also reached after sufficiently long thermal annealing.

Our results show that the complex kinetics of diffusion and adatom incorporation, and the interplay between the microscopic surface symmetry and the miscut azimuth can result in a metastable, mesoscopic morphology with a high degree of order both parallel and perpendicular to the miscut direction. Although the temperature range for triangle formation is remarkably narrow, it is close to the range where Si buffers are frequently deposited by MBE. Since nominal (001) Si substrates have typical miscut specifications of $\leq 0.5°$, it appears likely that such kinetic growth phenomena have accidentally affected subsequent heterostructure growth in the past. Preliminary experiments with 100 Å thick $Si_{0.8}Ge_{0.2}$ layers grown on top of a corrugated Si buffer as in Fig. 2(a) revealed perfect replication of the Si morphology. The implications for the transport of low-dimensional carriers bound to such an interface will be discussed elsewhere.

On the other hand, the observed ordering phenomena suggest new routes toward the fabrication of self-organized nanostructures: By careful adjustment of miscut angle and orientation, a highly periodic template can be prepared just by homoepitaxy. Self-assembled quantum dots in a subsequent heterolayer could then add the typical nanosize features associated with strain-driven phenomena, while maintaining the long range order of the template.

We thank J. Vanhellemont (Wacker Siltronic) and K. Brunner (WSI Munich) for providing vicinal Si(001) substrates, and J. Stangl for x-ray measurements of the miscuts. We acknowledge M. Pinczolits' help with the autocorrelation analyses, and valuable discussions with G. Bauer, B. Voigtländer, and P. Šmilauer. This work was financially supported by FWF (Project No. 12143 PHY), OeNB (Project No. 7333), and GMe.

[1] M. G. Lagally, Jpn. J. Appl. Phys. **32**, 1493 (1993).
[2] B. S. Swartzentruber, Y.-W. Mo, R. Kariotis, M. G. Lagally, and M. B. Webb, Phys. Rev. Lett. **65**, 1913 (1990).
[3] O. L. Alerhand, A. N. Berker, J. D. Joannopoulos, D. Vanderbilt, R. J. Hamers, and J. E. Demuth, Phys. Rev. Lett. **64**, 2406 (1990).
[4] U. Köhler, J. E. Demuth, and R. J. Hamers, J. Vac. Sci. Technol. A **7**, 2860 (1989).
[5] B. Voigtländer, T. Weber, P. Šmilauer, and D. E. Wolf, Phys. Rev. Lett. **78**, 2164 (1997).
[6] T. Whitaker and M. Meyer, Comp. Semicond. **4**, 30 (1998).
[7] See, e.g., G. Abstreiter, P. Schittenhelm, C. Engel, E. Silveira, A. Zrenner, D. Meertens, and W. Jäger, Semicond. Sci. Technol. **11**, 1521 (1996).
[8] F. Liu and M. G. Lagally, Surf. Sci. **386**, 169 (1997).
[9] J. Tersoff, Phys. Rev. Lett. **75**, 2730 (1995).
[10] See, e.g., F. Schäffler, Semicond. Sci. Technol. **12**, 1515 (1997).
[11] A. J. Pidduck, D. J. Robbins, and I. M. Young, Thin Solid Films **183**, 255 (1989).
[12] N. E. Lee, D. G. Cahill, and J. E. Greene, Phys. Rev. B **53**, 7876 (1996).
[13] S. Zerlauth, C. Penn, H. Seyringer, J. Stangl, G. Brunthaler, G. Bauer, and F. Schäffler, Thin Solid Films **321**, 33 (1998).
[14] Y. H. Phang, C. Teichert, M. G. Lagally, L. J. Peticolos, J. C. Bean, and E. Kasper, Phys. Rev. B **50**, 14 435 (1994).
[15] R. L. Schwoebel and E. J. Shipsey, J. Appl. Phys. **37**, 3682 (1966).
[16] G. S. Bales and A. Zangwill, Phys. Rev. B **41**, 5500 (1990).
[17] C. Roland and G. H. Gilmer, Phys. Rev. B **46**, 13 428 (1992); **46**, 13 437 (1992).
[18] Y.-W. Mo, J. Kleiner, M. B. Webb, and M. G. Lagally, Surf. Sci. **268**, 275 (1992).
[19] A. J. Hoeven, J. M. Lenssinck, D. Dijkkamp, E. J. van Loenen, and J. Dieleman, Phys. Rev. Lett. **63**, 1830 (1989).
[20] F. Wu, S. G. Jaloviar, D. E. Savage, and M. G. Lagally, Phys. Rev. Lett. **71**, 4190 (1993).
[21] Kinetic step bunching has also been observed on vicinal GaAs (110) surfaces; P. Tejedor, F. E. Allegretti, P. Šmilauer, and B. A. Joyce, Surf. Sci. **407**, 82 (1998).
[22] E. Kim, C. W. Oh, and Y. H. Lee, Phys. Rev. Lett. **79**, 4621 (1997).
[23] S. V. Ghaisas and S. Das Sarma, Phys. Rev. B **46**, 7308 (1992).
[24] E. Pehlke and J. Tersoff, Phys. Rev. Lett. **67**, 465 (1991).